Pt_3Ru_6 Clusters Supported on γ-Al_2O_3: Synthesis from $Pt_3Ru_6(CO)_{21}(\mu_3\text{-H})(\mu\text{-H})_3$, Structural Characterization, and Catalysis of Ethylene Hydrogenation and *n*-Butane Hydrogenolysis

Saowapa Chotisuwan,[†,‡,§] Jatuporn Wittayakun,[†] and Bruce C. Gates*[,§]

School of Chemistry, Suranaree University of Technology, Nakhon Ratchasima, Thailand, Department of Science, Prince of Songkla University, Pattani, Thailand, and Department of Chemical Engineering and Materials Science, University of California, Davis, California 95616

Received: December 28, 2005; In Final Form: April 22, 2006

The supported clusters Pt−Ru/γ-Al_2O_3 were prepared by adsorption of the bimetallic precursor $Pt_3Ru_6(CO)_{21}(\mu_3\text{-H})(\mu\text{-H})_3$ from CH_2Cl_2 solution onto γ-Al_2O_3 followed by decarbonylation in He at 300 °C. The resultant supported clusters were characterized by infrared (IR) and extended X-ray absorption fine structure (EXAFS) spectroscopies and as catalysts for ethylene hydrogenation and *n*-butane hydrogenolysis. After adsorption, the ν_{CO} peaks characterizing the precursor shifted to lower wavenumbers, and some of the hydroxyl bands of the support disappeared or changed, indicating that the CO ligands of the precursor interacted with support hydroxyl groups. The EXAFS results show that the metal core of the precursor remained essentially unchanged upon adsorption, but there were distortions of the metal core indicated by changes in the metal−metal distances. After decarbonylation of the supported clusters, the EXAFS data indicated that Pt and Ru atoms interacted with support oxygen atoms and that about half of the Pt−Ru bonds were maintained, with the composition of the metal frame remaining almost unchanged. The decarbonylated supported bimetallic clusters reported here are the first having essentially the same metal core composition as that of a precursor metal carbonyl, and they appear to be the best-defined supported bimetallic clusters. The material was found to be an active catalyst for ethylene hydrogenation and *n*-butane hydrogenolysis under conditions mild enough to prevent substantial cluster disruption.

Introduction

Supported catalysts incorporating two noble metals are important in technology. Examples include platinum catalysts modified by a second metal, including Pt−Ir supported on Al_2O_3 for naphtha reforming[1] and Pt−Rh supported on ceramic monoliths for automobile exhaust conversion.[2] Pt−Ru catalysts on carbon are used in hydrogen fuel cells for automotive applications.[3] The second metal in a combination, although it may be less active than the primary metal, may improve thermal stability and resistance to deactivation (as in Pt−Ir) of the catalyst as well as influencing catalytic activity and selectivity by affecting the metal surface composition and distribution of the atoms.[4,5]

Industrial bimetallic catalysts are prepared by deposition of two metal salts on a support. This conventional method is economical but results in particles or clusters of metal that are nonuniform in size, structure, and composition. It is difficult to prepare bimetallic catalysts in which the metals are not segregated. Molecular precursors, in contrast, allow control over the composition and structure of supported bimetallics.[6−9] Many potential bimetallic precursors, however, are unattractive because they incorporate stabilizing ligands (e.g., phosphines) that remain on the metal or the support after activation and act as catalyst poisons and complicate structural characterization of the metal species. Thus, it is advantageous to use precursors incorporating only ligands such as hydride, alkyl, and CO, which may be readily removed without substantial disruption of the metal frame.

Such precursors include the family of Pt−Ru clusters, exemplified by $Pt_2Ru_4(CO)_{18}$, $PtRu_5C(CO)_{16}$, and $Pt_3Ru_6(CO)_{21}(\mu_3\text{-H})(\mu\text{-H})_3$.[10−13] Supported catalysts have been prepared from all but the last of these precursors. The local environments around the metal atoms in the supported samples can be characterized by extended X-ray absorption fine structure (EXAFS) spectroscopy.[8,14] The available data show that after adsorption of the precursor clusters on carbon supports followed by decarbonylation, the resultant supported clusters were usually larger than the metal core of the precursor, indicating that aggregation had occurred.[15−17] In contrast, when the precursor $Pt_2Ru_4(CO)_{18}$ was adsorbed on γ-Al_2O_3, EXAFS spectra showed that the average decarbonylated cluster contained less than about nine metal atoms, indicating that aggregation had occurred, but to a markedly smaller degree than in the carbon-supported samples.[6]

In an attempt to prepare uniform and well-defined supported Pt−Ru clusters, we used a cluster precursor−support combination affording the opportunity to adsorb the precursor intact and remove the ligands with minimal disruption of the metal frame. $Pt_3Ru_6(CO)_{21}(\mu_3\text{-H})(\mu\text{-H})_3$ was chosen to be the precursor because it was expected to have a high reactivity with the support γ-Al_2O_3, associated with its hydride ligands.

The crystal structure of the cluster has been determined and shown to incorporate three triangular layers consisting of nine metal atoms arranged in the form of a face-shared bi-

* Corresponding author. E-mail: bcgates@ucdavis.edu.
[†] Suranaree University of Technology.
[‡] Prince of Songkla University.
[§] University of California.

10.1021/jp057550+ CCC: $33.50
Published on Web 06/06/2006

octahedron.[13] The middle layer of the cluster core contains three Pt atoms shared by the first and third layer consisting of three Ru atoms each. One triruthenium face incorporates three hydride ligands, one bridged to each edge, and another hydride ligand is triply bridged to the other triangular Ru_3 face. The hydride ligands could be replaced by PhC_2Ph (Ph is phenyl) and transferred to an alkyne, thus forming an alkene, a result that indicates that the hydride ligands could be removed easily. Removal of the hydride ligands from this precursor on the surface of a support is expected to allow relatively strong cluster−support interactions, stabilizing the supported clusters. One of our goals was to test the hypothesis that the removal of carbonyl ligands from such precursors stabilized on a support would result in supported Pt_3Ru_6 clusters that were freed of ligands and catalytically active.

We now report the synthesis of a supported catalyst containing bimetallic clusters nearly matching the frame of the precursor $Pt_3Ru_6(CO)_{21}(\mu_3\text{-H})(\mu\text{-H})_3$. Changes of the supported species after the precursor adsorption on γ-Al_2O_3 and after subsequent decarbonylation were monitored by infrared (IR) and EXAFS spectroscopies. The decarbonylated samples were evaluated as catalysts for ethylene hydrogenation and *n*-butane hydrogenolysis under conditions mild enough to minimize the likelihood of disruption of the cluster frames.

Experimental Methods

Reagents and Materials. γ-Al_2O_3 powder (Degussa, BET surface area approximately 100 m^2/g) was calcined in flowing O_2 at 400 °C for 2 h and evacuated (pressure $\approx 10^{-3}$ Torr) for 14 h before use. *n*-Hexane and *n*-pentane solvents (Fisher, 99%) were distilled over Na/benzophenone and purged with N_2 to remove O_2. Dichloromethane (CH_2Cl_2) solvent (Fisher, >99.5%) was dried over a 4A molecular sieve to remove traces of water and deoxygenated with N_2 before use. Gases [He (Airgas, 99.99%), Ar (Airgas, 99.99%), C_2H_4 (Matheson, 99.5%), *n*-C_4H_{10} (Airgas, 99.5%), and H_2 (Matheson, 99.999% or formed by electrolysis of water in a Balston H_2 generator, 99.99%)] were purified by passage through traps containing reduced Cu/Al_2O_3 and activated zeolite particles to remove traces of O_2 and water.

Preparation of Cluster Precursor. $Pt_3Ru_6(CO)_{21}(\mu_3\text{-H})(\mu\text{-H})_3$ was synthesized from $Pt_2Ru_4(CO)_{18}$ and H_2 at 97 °C and purified by washing with cold *n*-pentane.[13] Its structure and purity were confirmed by ^1H and ^{13}C NMR spectroscopy with the sample in acetone-d_6 at −88 °C and by IR spectroscopy with the sample in CH_2Cl_2.

Preparation of Pt−Ru/γ-Al_2O_3 Catalysts. The supported clusters (referred to as Pt−Ru/γ-Al_2O_3) containing 1.0 wt % Pt and 1.0 wt % Ru were prepared by slurrying $Pt_3Ru_6(CO)_{21}(\mu_3\text{-H})(\mu\text{-H})_3$ in CH_2Cl_2 with γ-Al_2O_3 powder for 1 day. After removal of the CH_2Cl_2 solvent by evacuation for 1 day, the dried solid sample containing adsorbed clusters was characterized by IR spectroscopy. To transform the supported clusters into the catalytically active form, the sample was treated in flowing He at 300 °C for 2 h to remove ligands; it was then characterized again by IR spectroscopy.

Extraction of Adsorbed Species. After solvent removal from the γ-Al_2O_3-adsorbed bimetallic cluster precursor by evacuation, the adsorbed species were recovered by extraction with CH_2Cl_2 for approximately 30 min with continuous stirring. After filtration and drying, the extract solution and the extracted dry sample were characterized by IR spectroscopy.

IR Spectroscopy. IR spectra were recorded with a Bruker IFS-66v spectrometer with a resolution of 4 cm^{-1}. Each sample was scanned 64 times, and the signal was averaged.

EXAFS Spectroscopy. EXAFS experiments were performed at X-ray beamline X-18B at the National Synchrotron Light Source (NSLS), Brookhaven National Laboratory, Upton, New York. The storage ring energy was 2.5 GeV, and the ring current was in the range of 110−250 mA. Each sample (0.3 g) was pressed into a self-supporting wafer with an approximate thickness of 0.3 mm in an Ar-filled glovebox at the synchrotron, placed in a holder, and mounted in a cell.[18] The cell was evacuated, installed at the beamline, and cooled to nearly liquid-nitrogen temperature. The sample was scanned at the Pt L_{III} edge (11564 eV) and the Ru K edge (22117 eV) in transmission mode, with integration for 1 s at each energy in the range from 200 eV below the absorption edge to 975 eV beyond the edge. A double-crystal Si(111) monochromator was used. Details of the EXAFS measurements are as reported elsewhere.[19]

Catalytic Activity of PtRu/γ-Al_2O_3 for Ethylene Hydrogenation. The ethylene hydrogenation experiments were carried out with 10−20 mg of pretreated catalyst diluted with 600 mg of inert, nonporous α-Al_2O_3 powder in a stainless steel U-tube flow reactor operated at atmospheric pressure. Each sample was pretreated in flowing He or H_2 at 300 °C for 2 h, loaded into the reactor in an Ar-filled glovebox, isolated from air and moisture, and transferred to the flow reactor system. With the sample in flowing He, the reactor was cooled to the desired temperature, whereupon flow of a gas mixture of H_2, C_2H_4, and He was started at a rate of 100 mL (NTP)/min. The effluent gas mixture was analyzed with an online gas chromatograph (Hewlett-Packard HP 6890) equipped with an Al_2O_3 capillary column (50 m × 0.53 nm × 15.0 μm film thickness) and a flame ionization detector. Catalytic reactions were carried out with the partial pressures $P_{H_2} = 200$ Torr and $P_{C_2H_4} = 40$ Torr, with the remainder being He and the pressure atmospheric; the catalytic reaction temperature was varied from −50 to −5 °C.

Catalytic Activity of PtRu/γ-Al_2O_3 for *n*-Butane Hydrogenolysis. The activity of the catalyst was determined for *n*-butane hydrogenolysis. A blank test was carried with feed to a quartz-tube reactor packed with inert, nonporous α-Al_2O_3 under the following conditions, giving no evidence of reaction in the absence of the supported bimetallic catalyst: $P_{H_2} = 540$ Torr, $P_{n\text{-}C_4H_{10}} = 60$ Torr; feed flow rate = 100 mL (NTP)/min; and reactor temperature = 220 °C.

In an Ar-filled glovebox, approximately 30 mg of catalyst sample was mixed with inert, nonporous α-Al_2O_3, loaded into the reactor, and isolated from air and moisture before being transferred to the flow reactor system. The reactor was heated to the desired temperature with He flowing through it before the start of flow of a mixture containing H_2, *n*-C_4H_{10}, and He at a rate of 100 mL (NTP)/min. The effluent gas mixture was analyzed with the online gas chromatograph equipped with the column mentioned above. The reaction conditions were as follows: $P_{H_2} = 540$ Torr, $P_{n\text{-}C_4H_{10}} = 60$ Torr, with the temperature varied from 190 to 260 °C.

EXAFS Data Analysis

The four sets of raw EXAFS data characterizing each sample were averaged with the software ATHENA developed by Raval[20] and analyzed with the software EXAFSPAK developed by George et al.[21] The phase shifts and backscattering amplitudes characterizing Pt−Pt, Pt−Ru, Pt−$O_{support}$, Ru−Ru, Ru−Pt, and Ru−$O_{support}$ interactions were calculated with the software FEFF7.0.[22] The EXAFS data fitting was carried out with EXAFSPAK[21] with single and multiple scattering paths calculated with FEFF7.0.[22] Fitting was done both in *r* space (*r* is the distance from the absorber atom, Pt or Ru) and *k* space (*k* is

the wave vector) with application of k^0, k^1, and k^3 weightings until excellent agreement between the fit for each of the k weightings and the data was attained. The Pt−Al and Ru−Al contributions could not be determined with confidence because these are small and not uniquely defined, because the nonuniformity of the support surface results in various cluster−support interactions. Others have reported that the errors in metal−Al contributions were large (when the metal was Rh or Ir);[23,24] Many authors reporting similar data have simply omitted such contributions from their fits of EXAFS data.

The EXAFS Pt L_{III}-edge data characterizing the supported clusters prepared from $Pt_3Ru_6(CO)_{21}(\mu_3\text{-H})(\mu\text{-H})_3$ before decarbonylation were Fourier-transformed over the ranges $3.56 < k < 12.85$ Å^{-1} with k^3 weighting without phase correction and $0.0 < r < 5.0$ Å. The data characterizing this sample at the Ru K edge were Fourier-transformed over the ranges $4.25 < k < 14.50$ Å^{-1} and $0.0 < r < 4.0$ Å. The statistically justified numbers of free parameters estimated from the Nyquist theorem[25] for the Pt L_{III} and Ru K edges were approximately 31 and 27, respectively.

The Pt L_{III}-edge EXAFS data characterizing the supported clusters after decarbonylation in He were Fourier-transformed over the ranges $3.25 < k < 14.25$ Å^{-1} and $0.0 < r < 5.0$ Å. The data at the Ru K edge were Fourier-transformed over the ranges $3.40 < k < 14.45$ Å^{-1} and $0.0 < r < 4.0$ Å. The statistically justified number of free parameters estimated from the Nyquist theorem at the Pt L_{III} and Ru K edges were approximately 36 and 29, respectively.

Results

Structural Characterization of the Cluster Precursor in Solution. The structure of $Pt_3Ru_6(CO)_{21}(\mu_3\text{-H})(\mu\text{-H})_3$ was confirmed by ^{1}H and ^{13}C NMR spectroscopy and by IR spectroscopy. The NMR data matched those reported:[13] The hydride peaks in the ^{1}H NMR spectrum were observed at −15.84 and −19.28 ppm in a 3:1 ratio; the carbonyl carbon was observed in the ^{13}C NMR spectrum at 190.28 ppm. The IR spectrum of the cluster in the ν_{CO} region (Figure 1a) includes peaks at 2081(sh), 2065(s), 2048(m), and 2023(w) cm^{-1}.

Because IR spectroscopy could be used to characterize samples both in solution and in the solid state, it was an important tool for investigation of changes of the precursor at each step of catalyst preparation.

Structural Characterization of Metal Carbonyls Initially Formed on Support. After slurrying of the cluster dissolved in CH_2Cl_2 with γ-Al_2O_3, the cluster's dark brown color disappeared slowly as the solid darkened, consistent with the cluster's being adsorbed on the γ-Al_2O_3. After stirring for 1 day, the brown color characterizing of the cluster in solution had become very light, indicating that almost all of it had been adsorbed.

The spectrum of the sample consisting of the adsorbed precursor on γ-Al_2O_3 after drying is shown in Figure 1b, spectrum 1. The spectrum of the adsorbed precursor is similar to that of the precursor in solution (Figure 1a), but the peaks are broadened and shifted, to 2073(w, sh), 2038(s), and 2011-(w, sh) cm^{-1}. The existence of the ν_{CO} bands confirms that the adsorbed species were still metal carbonyls; the shifting and broadening of these bands indicate changes of the C−O bond strength after metal atoms in the precursor interacted with oxygen atoms of the nonuniform support surface.[26] Such interactions resulted in more back-bonding from metal to π^* antibonding orbitals of carbonyl carbon and weakened the C−O bond. The similarity of the spectral shape to that of the precursor

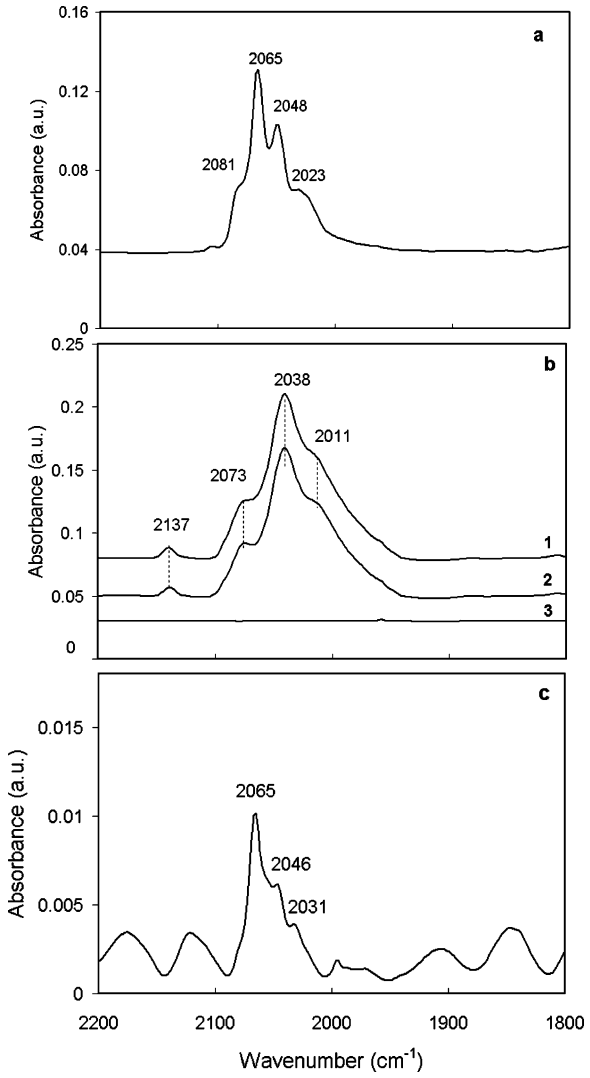

Figure 1. (a) IR spectra in ν_{CO} region of a solution of $Pt_3Ru_6(CO)_{21}(\mu_3\text{-H})(\mu\text{-H})_3$ in CH_2Cl_2. (b) IR spectra in ν_{CO} region: (1) Dry supported sample after adsorption of $Pt_3Ru_6(CO)_{21}(\mu_3\text{-H})(\mu\text{-H})_3$ on γ-Al_2O_3; (2) dry supported sample after extraction with CH_2Cl_2; (3) PtRu/γ-Al_2O_3 after decarbonylation. (c) IR spectrum of extract solution after extraction of the supported sample with CH_2Cl_2.

indicates the lack of significant changes in structure of the cluster as a result of adsorption.

After the adsorbed species on γ-Al_2O_3 had been brought in contact with CH_2Cl_2 and the solid had been dried by evacuation, it still had an IR spectrum similar to that of the sample before contacting with CH_2Cl_2 (Figure 1b, spectrum 2), indicating that the precursor was chemisorbed on the support and barely changed as a result of the attempted extraction. The peaks representative of the solvent CH_2Cl_2 (at 2988 and 3060 cm^{-1}) were absent from the spectrum (not shown), indicating that its adsorption was negligible.

Information about the extracted species is given in the following section.

A weak peak at 2137 cm^{-1} was observed in the spectrum of the supported precursor, both before and after the attempted extraction; this might be assigned to small amounts of supported Pt^{2+}−CO or Pt^{+}−CO species formed from the bimetallic clusters; peaks characterizing such species have been observed in the range of 2135−2110 cm^{-1}.[27,28] Furthermore, there was a weak, broad band at 1589 cm^{-1}, suggesting the coordination of some clusters to surface Al^{3+} ions (Lewis acid sites) of the γ-Al_2O_3.[29]

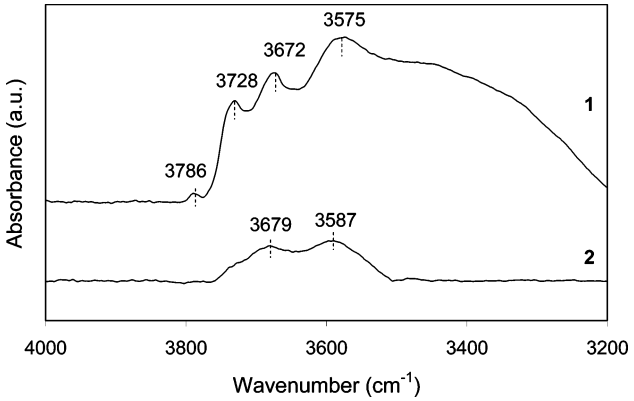

Figure 2. IR spectra in ν_{OH} region: (1) bare γ-Al_2O_3 calcined at 400 °C for 14 h; (2) dried sample prepared from $Pt_3Ru_6(CO)_{21}(\mu_3\text{-H})(\mu\text{-H})_3$ and γ-Al_2O_3.

Treatment of the supported metal carbonyl in He at 300 °C for 2 h led to essentially complete decarbonylation, indicated by the disappearance of all of the carbonyl bands (Figure 1b, spectrum 3).

Extraction of Adsorbed Metal Carbonyl Precursors. After 30 min of contact of the supported metal carbonyl clusters with CH_2Cl_2, the ν_{CO} peaks remained essentially unchanged, indicating that the supported clusters were strongly adsorbed, but the extract solution had very light brown color similar to that of the solution after the initial adsorption step. This observation shows that a small amount of the adsorbed precursor was extracted into CH_2Cl_2. The ν_{CO} spectrum of the extract solution was characterized by three low-intensity peaks, at 2065(s), 2046(m), and 2031(w) cm^{-1} (Figure 1c); the spectrum is similar to that of the precursor in solution, except that the shoulder at 2081 cm^{-1} was barely observed.

Evidence of Reaction of Cluster Precursor with γ-Al_2O_3. Consistent with bonding of OH groups of the support to the metal carbonyl, the IR bands in the ν_{OH} region of the spectrum characteristic of bare γ-Al_2O_3 at 3786 and 3728 cm^{-1} (Figure 2, spectrum 1) decreased in intensity after adsorption of the metal carbonyl cluster (Figure 2, spectrum 2), consistent with reaction of the support OH groups with the cluster during the adsorption. (The IR spectra comparing the bare γ-Al_2O_3 and that with adsorbed precursor are not quantitatively comparable, because separate samples with different thicknesses were used.)

The bands at 3786(w), 3728(m), and 3672(m) have been assigned to isolated surface OH groups, and the broad absorption centered at 3575 cm^{-1} has been assigned to hydrogen-bonded OH groups.[30,31] The only bands in the ν_{OH} region remaining after adsorption of the cluster were observed at 3679(w) cm^{-1} (representing isolated OH groups[30]) and 3587(w) cm^{-1} (representing hydrogen-bonded OH groups).[30,31] Thus, we infer that the cluster precursor reacted principally with isolated surface OH groups of the support.

XANES Data Characterizing Supported Sample Before and After Decarbonylation. The raw XAS data characterizing the supported clusters prepared from $Pt_3Ru_6(CO)_{21}(\mu_3\text{-H})(\mu\text{-H})_3$ before and after decarbonylation, showing changes at the Pt L_{III} and Ru K edges, are presented in Figure 3a and b, respectively. These data are similar to those characterizing the respective metal foils and indicate the metals in oxidation states near zero, but further statements are not justified.

EXAFS Data Characterizing Adsorbed Metal Carbonyl Clusters. The normalized and Fourier-transformed EXAFS data are shown in Figure 4 (solid line), along with the fits (dotted line). The data at the Pt L_{III} and Ru K edges (Figure 4A and C,

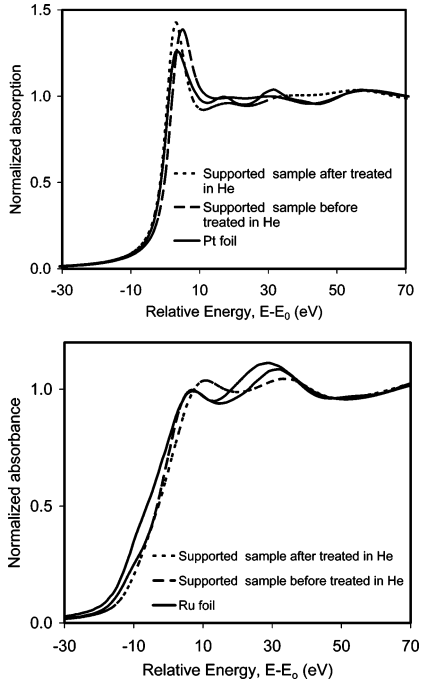

Figure 3. (top) XANES spectra scanned at Pt L_{III} edge characterizing the γ-Al_2O_3-supported PtRu sample prepared by adsorption of $Pt_3Ru_6(CO)_{21}(\mu_3\text{-H})(\mu\text{-H})_3$ before and after treatment in He at 300 °C compared with Pt foil. (bottom) XANES spectra scanned at Ru K edge characterizing the γ-Al_2O_3-supported PtRu sample prepared by adsorption of $Pt_3Ru_6(CO)_{21}(\mu_3\text{-H})(\mu\text{-H})_3$ before and after treatment in He at 300 °C compared with Ru foil.

respectively) show oscillations up to values of k of approximately 13 and 15 $Å^{-1}$, respectively, indicating the presence of near-neighbor high-Z backscatterers around the Pt and Ru atoms.

A self-consistent EXAFS analysis requires that the bond distances and Debye−Waller factors representing the Pt−Ru interactions be equivalent in the fits determined at each metal edge; furthermore, the corresponding coordination number, N_{PtRu}, must be related to N_{RuPt} as follows: $N_{PtRu}/N_{RuPt} = n_{Ru}/n_{Pt}$, where n_{Ru} and n_{Pt} are the total numbers of Ru and Pt atoms in sample.[4−6] These constraints were applied in the data fitting. The resultant EXAFS parameters are summarized in Table 1.

The EXAFSPAK software[21] was used to obtain estimates of the error bounds in these parameters (Tables 1). The error bounds represent precisions determined from statistical analysis of the data from the multiple scans, not accuracies. The estimated accuracies of the EXAFS parameters (and those reported below) characterizing the metal−metal contributions are approximately as follows: coordination number N, ±20%; distance R, ±1%; Debye−Waller factor $\Delta\sigma^2$, ±30%; and inner potential correction ΔE_0, ±10%; the accuracies of the metal−oxygen contributions are somewhat less.

The EXAFS results of Table 1 include coordination numbers and distances of metal−metal (Pt−Pt, Pt−Ru, Ru−Pt, and Ru−Ru); metal−carbonyl carbon (Pt−C, Ru−C); and metal−support ($Pt-O_{support}$, $Ru-O_{support}$) bonds, as well as of Pt−O* and Ru−O* contributions, where O* represents carbonyl oxygen. The metal−metal coordination numbers (Table 1) are consistent with the inference that the cluster core of adsorbed precursor, although distorted, remained essentially intact.

Table 1 includes a comparison of the EXAFS-determined bond distances and coordination numbers of the adsorbed precursor on γ-Al_2O_3 with the crystallographic data characterizing $Pt_3Ru_6(CO)_{21}(\mu_3\text{-H})(\mu\text{-H})_3$.[13] The average Pt−Pt bond

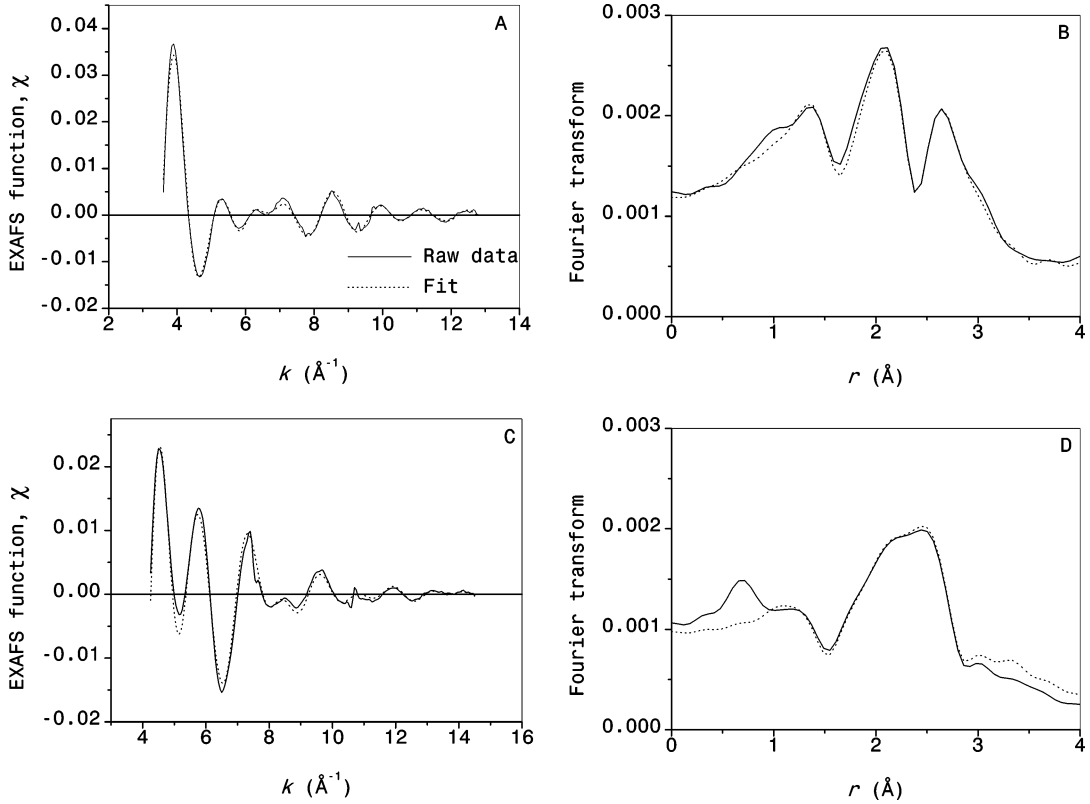

Figure 4. EXAFS results scanned at Pt L_{III} edge and at Ru K edge characterizing the γ-Al_2O_3-supported PtRu sample prepared by adsorption of $Pt_3Ru_6(CO)_{21}(\mu_3\text{-H})(\mu\text{-H})_3$: (A) Experimental EXAFS function (solid line) and sum of the calculated Pt−Pt, Pt−Ru, Pt−C, Pt−O*, Pt−O_s, and Pt−O_l contributions (dotted line). (B) Magnitude of uncorrected Fourier transform (k^0 weighted) of experimental EXAFS function (solid line) and sum of the calculated Pt−Pt, Pt−Ru, Pt−C, Pt−O*, Pt−O_s, and Pt−O_l contributions (dotted line). (C) Experimental EXAFS function (solid line) and sum of the calculated Ru−Ru, Ru−Pt, Ru−C, Ru−O*, Ru−O_s, and Ru−O_l contributions (dotted line). (D) Magnitude of uncorrected Fourier transform (k^0 weighted) of experimental EXAFS function (solid line) and sum of the calculated Ru−Ru, Ru−Pt, Ru−C, Ru−O*, Ru−O_s, and Ru−O_l contributions (dotted line).

TABLE 1: Summary of Structural Data Characterizing Crystalline $Pt_3Ru_6(CO)_{21}(\mu_3\text{-H})(\mu\text{-H})_3$,[13] Supported Species Formed from this Cluster on γ-Al_2O_3, and Sample after Adsorption of $Pt_3Ru_6(CO)_{21}(\mu_3\text{-H})(\mu\text{-H})_3$ on γ-Al_2O_3[a]

		XRD[13] data characterizing $Pt_3Ru_6(CO)_{21}(\mu_3\text{-H})(\mu\text{-H})_3$		EXAFS data characterizing sample formed by adsorption of $Pt_3Ru_6(CO)_{21}(\mu_3\text{-H})(\mu\text{-H})_3$ on γ-Al_2O_3				EXAFS data characterizing sample formed by adsorption of $Pt_3Ru_6(CO)_{21}(\mu_3\text{-H})(\mu\text{-H})_3$ on γ-Al_2O_3 after treatment in He at 300 °C for 2 h			
edge	shell	N	R (Å)	N	R (Å)	$10^3 \times \Delta\sigma^2$ (Å^2)	ΔE_0 (eV)	N	R (Å)	$10^3 \times \Delta\sigma^2$ (Å^2)	ΔE_0 (eV)
Pt L_{III}	Pt−Pt	2.0	2.64	2.2 ± 0.1	2.68 ± 0.01	6.4 ± 0.3	2.7 ± 0.1	1.7 ± 0.2	2.64 ± 0.01	3.0 ± 0.7	−4.5 ± 0.8
	Pt−Ru	4.0	2.80	3.9 ± 0.1	2.95 ± 0.01	6.9 ± 0.1	−8.2 ± 0.1	2.2 ± 0.1	2.68 ± 0.01	4.2 ± 0.5	6.0 ± 0.3
	Pt−CO										
	Pt−C	1.0	1.85	0.8 ± 0.1	1.85 ± 0.01	−0.1 ± 0.4	6.2 ± 0.3				
	Pt−O*	1.0	2.99	0.8 ± 0.1	3.09 ± 0.01	−10.9 ± 0.1	10.6 ± 0.2				
	Pt−$O_{support}$										
	Pt−O_s			1.8 ± 0.1	2.55 ± 0.01	0.7 ± 0.2	−0.6 ± 0.1	2.2 ± 0.1	2.08 ± 0.01	11.3 ± 1.4	8.7 ± 0.6
	Pt−O_l			2.3 ± 0.1	3.05 ± 0.01	-7.3 ± 0.1	19.2 ± 0.1	0.8 ± 0.1	2.99 ± 0.02	−2.3 ± 2.0	−7.6 ± 1.4
Ru K	Ru−Ru	2.0	3.04	1.9 ± 0.1	2.83 ± 0.01	12.5 ± 0.6	7.1 ± 0.2	2.1 ± 0.1	2.62 ± 0.01	4.1 ± 0.3	−13.3 ± 0.3
	Ru−Pt	2.0	2.80	2.0 ± 0.1	2.95 ± 0.01	7.0 ± 0.5	9.9 ± 0.3	1.0 ± 0.1	2.68 ± 0.01	4.5 ± 0.7	−11.5 ± 1.0
	Ru−CO										
	Ru−C	3.0	1.89	3.1 ± 0.1	1.88 ± 0.01	3.8 ± 0.2	−4.3 ± 0.3				
	Ru−O*	3.0	3.03	3.1 ± 0.1	3.00 ± 0.01	1.6 ± 0.3	−1.4 ± 0.2				
	Ru−$O_{support}$										
	Ru−O_s			1.4 ± 0.1	2.34 ± 0.01	9.3 ± 0.7	12.3 ± 0.2	1.2 ± 0.1	2.06 ± 0.01	10.9 ± 1.7	4.1 ± 0.7
	Ru−O_l			0.6 ± 0.1	3.40 ± 0.01	−2.1 ± 1.2	16.2 ± 0.5	2.1 ± 0.1	2.89 ± 0.01	0.1 ± 0.7	11.8 ± 0.2

[a] Notation: O* refers to carbonyl oxygen; O_s and O_l refer to support oxygen at short and long distances, respectively.

length in the chemisorbed cluster (2.68 ± 0.01 Å) is slightly greater than that in the crystalline precursor (average, 2.64 Å), but the average Pt−Ru bond length in the chemisorbed cluster (2.95 ± 0.01 Å) is markedly greater than that in the crystalline precursor (average value, 2.80 Å). The average Ru−Ru bond length in the adsorbed species (2.83 ± 0.01 Å) is markedly less than that in the precursor (average value, 3.04 Å). These results indicate distortion of the cluster frame upon adsorption.

The average distances between Pt (or Ru) atoms and the carbon atom of the carbonyl ligands in the adsorbed species nearly match those in the precursor. The Pt−O* distance is 0.1 Å greater than that of the precursor, and the Ru−O* distance

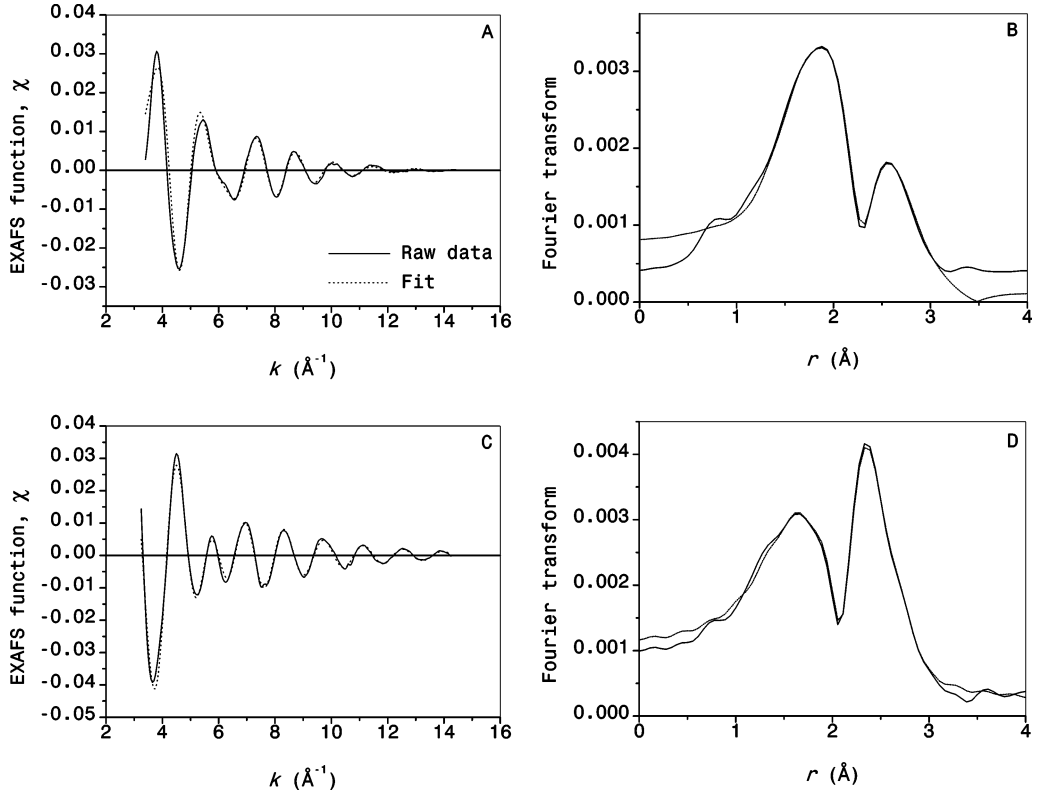

Figure 5. EXAFS results scanned at Pt L_{III} edge and at Ru K edge characterizing the γ-Al_2O_3-supported PtRu sample prepared by adsorption of $Pt_3Ru_6(CO)_{21}(\mu_3\text{-H})(\mu\text{-H})_3$ followed by treatment in He. (A) Experimental EXAFS function (solid line) and sum of the calculated Pt−Pt, Pt−Ru, Pt−O_s, and Pt−O_l contributions (dotted line). (B) Magnitude of uncorrected Fourier transform (k^0 weighted) of experimental EXAFS function (solid line) and sum of the calculated Pt−Pt, Pt−Ru, Pt−O_s, and Pt−O_l contributions (dotted line). (C) Experimental EXAFS function (solid line) and sum of the calculated Ru−Ru, Ru−Pt, Ru−O_s, and Ru−O_l contributions (dotted line). (D) Magnitude of uncorrected Fourier transform (k^0 weighted) of experimental EXAFS function (solid line) and sum of the calculated Ru−Ru, Ru−Pt, Ru−O_s, and Ru−O_l contributions (dotted line).

is barely different from that of the precursor. The data give evidence of interactions between the metal and support oxygen atoms, characterized by a Pt−O_s distance (s refers to short) of 2.55 ± 0.01 Å (with a coordination number of 1.8 ± 0.1) and a Ru−O_s distance of 2.34 ± 0.01 Å (with a coordination number 1.4 ± 0.1). These data provide evidence of strong metal−support interactions, which presumably helped to induce the aforementioned distortions in the metal frame and changes in the metal−CO bonding.

EXAFS Data Characterizing Decarbonylated Clusters on Support. The normalized and Fourier-transformed EXAFS data and the corresponding fits representing the supported PtRu clusters after decarbonylation are shown in Figure 5. The data scanned at the Pt L_{III} and Ru K edges (Figure 5A and C) show oscillations at values of k of as much as about 13 and 14 $Å^{-1}$, respectively, indicating the presence of near-neighbor high-Z backscatterers around Pt and Ru atoms. The relatively weak oscillations in the high-k regions indicate the absence of large (aggregated) metal clusters in the sample.

Table 1 also includes a summary of the EXAFS results characterizing the metal−metal (Pt−Pt, Pt−Ru, Ru−Pt, and Ru−Ru) and metal−support contributions (Pt−$O_{support}$ and Ru−$O_{support}$). Each of the metal−metal bonds after ligand removal from the supported clusters was shorter than that characterizing the adsorbed precursor. Although the Pt−Pt and Ru−Ru coordination numbers did not change significantly upon decarbonylation, the Pt−Ru and Ru−Pt coordination numbers decreased to approximately half of the initial values. The clear evidence of Pt−Ru bonds (based on data at both metal edges) demonstrates that intact bimetallic PtRu clusters were prepared successfully from the bimetallic precursor.

Furthermore, the EXAFS data confirm the IR data in showing that the decarbonylation was essentially complete because neither Pt−C nor Ru−C contributions were observed for the sample treated in He.

The values of the metal−metal coordination numbers show that the decarbonylated clusters on the support were similar in size to the metal frame of the precursor.

Models of the supported clusters consistent with these coordination numbers are shown in Table 2. The models were constructed on the basis of the metal−metal coordination numbers obtained in the analysis of the EXAFS data, with errors of approximately ±20%. For simplification in construction of the models, the atomic sizes of Pt and Ru were assumed to be the same, and the interactions between metal and support oxygen were not included.

Catalytic Activity of Supported Bimetallic Clusters for Ethylene Hydrogenation. In the catalytic reaction experiments with ethylene and H_2 as the feeds, the only observed product was ethane. The conversions of ethylene and H_2 fluctuated around 11.0% at the first 50 min time on stream (TOS) at the temperature −40 °C and became nearly constant at 10.0% for the duration of the testing (up to 110 min TOS). The catalytic activities in terms of turnover frequency (TOF) and the temperature dependence of TOF (the apparent activation energy, E_{app}) of these PtRu catalysts and other Pt catalysts are compared in Table 3. TOF was calculated on the basis of the inference from the EXAFS data that essentially all of the metal atoms in the clusters were accessible to reactants. (The calculation ignores any lack of accessibility of Pt or Ru atoms resulting from their nearness to the support.) The rate data are summarized in the Arrhenius plots of Figure 6.

TABLE 2: Top View of Models of Bimetallic Clusters on γ-Al_2O_3 Prepared from $Pt_3Ru_6(CO)_{21}(\mu_3\text{-H})(\mu\text{-H})_3$ after Treatment in He at 300 °C for 2 h Based on EXAFS Metal−Metal Coordination Numbers[a]

Structure	Proposed cluster models	*N*
(I)	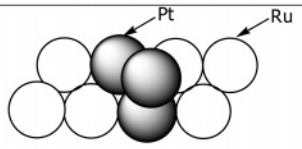	Pt–Pt = 2 Pt–Ru = 2.3 Ru–Ru = 2 Ru–Pt = 1.2
(II)	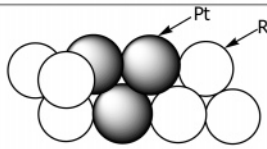	Pt–Pt = 2 Pt–Ru = 2.3 Ru–Ru = 2 Ru–Pt = 1.2
(III)	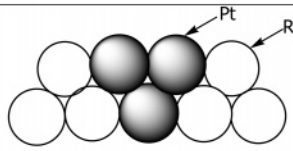	Pt–Pt = 2 Pt–Ru = 2 Ru–Ru = 2 Ru–Pt = 1
(IV)	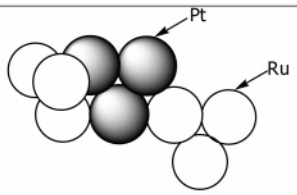	Pt–Pt = 2 Pt–Ru = 2 Ru–Ru = 2 Ru–Pt = 1
(V)	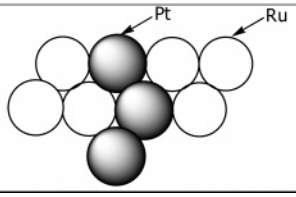	Pt–Pt = 1.3 Pt–Ru = 2.3 Ru–Ru = 2 Ru–Pt = 1.2

[a] The estimated errors in the coordination number (*N*) are ±20%.

TABLE 3: Activities of Ethylene Hydrogenation Catalysts: Supported PtRu and Pt Clusters[a]

precursor(s)	support	activity, turnover frequency × 10^4 (s^{-1}) at −40 °C	E_{app} (kcal/mol)	temperature (°C)	refs
$Pt_3Ru_6(CO)_{21}(\mu_3\text{-H})(\mu\text{-H})_3$	γ-Al_2O_3	12.2 ± 1.0	7.4 ± 0.1	−40 to −5	this work
$Pt(acac)_2 + Ru(acac)_3$	γ-Al_2O_3	15.4 ± 0.4	8.1 ± 0.1	−50 to −10	36
$Pt(cod)Cl_2 + Ru(cod)Cl_2$	γ-Al_2O_3	6.8 ± 0.2	6.7 ± 0.1	−50 to −10	36
$RuPt_2(CO)_5(PPh_3)_3$	functionalized cross-linked polystyrene		7.8 ± 1.2	73 to 98	37
Pt vapor	Al_2O_3		10.2 ± 0.2	40 to 150	38, 39

[a] Notation: E_{app}, apparent activation energy; cod, 1,5-cyclooctadiene; Ph, phenyl.

Catalytic Activity of Supported Bimetallic Clusters for *n*-Butane Hydrogenolysis. The products of the reaction of *n*-butane and H_2 were methane, ethane, and propane, consistent with the occurrence of catalytic hydrogenolysis of *n*-butane. The conversions of *n*-butane and H_2 ranged from 0.5 to 41.1% for temperatures in the range of 190 to 260 °C. The activity of the catalyst is represented as the average TOF calculated from conversions to methane, ethane, and propane presuming that they were differential; this is only an approximation for the higher conversions.

Figure 7 shows that *n*-butane hydrogenolysis activity at temperatures in the range of 190−260 °C increased with temperature. There was almost no activity at 200 °C. At this temperature, the conversion increased slowly with TOS in the flow reactor and became constant at about 1.1% after 60 min. At 260 °C, the conversion became approximately 20% after 160 min TOS, and then it remained nearly constant for the whole duration of the experiment (250 min TOS) with temperatures varied in the range of 190−260 °C. These results imply that catalyst deactivation such as might be caused by aggregation of metal particles or coking did not occur significantly during the catalytic tests.

The catalytic activity in terms of TOF at 220 °C was found to be $(5.2 \pm 0.2) \times 10^{-4}$ s^{-1}. The product distribution data are shown in Figure 8. As the temperature increased, the amount of ethane, propane, and *iso*-butane decreased, becoming almost independent of temperature at temperatures higher than 220 °C. In contrast, the selectivity for methane increased as the temperature increased, becoming almost independent of temperature at temperatures higher than 220 °C. An Arrhenius plot (Figure 9) shows the temperature dependence of the approximate TOF values, with the data obtained at ascending temperatures in the range of 190 to 260 °C; the apparent activation energy was found to be 30.9 kcal/mol.

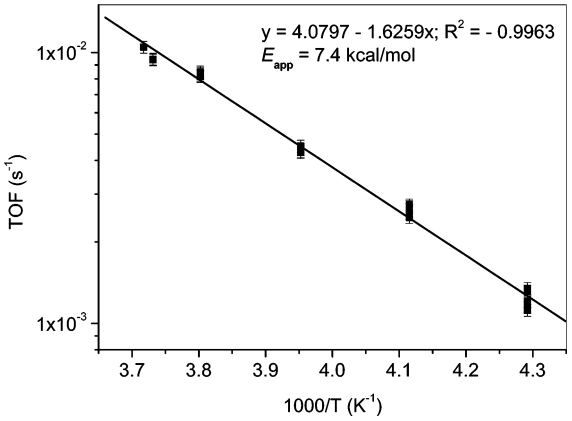

Figure 6. Arrhenius plot representing ethylene hydrogenation catalyzed by PtRu/γ-Al_2O_3 samples prepared from adsorption of $Pt_3Ru_6(CO)_{21}(\mu_3\text{-H})(\mu\text{-H})_3$.

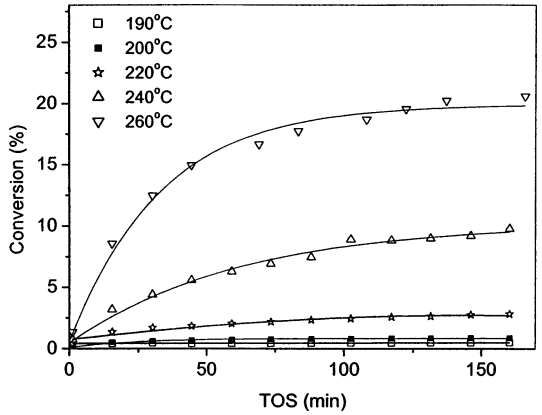

Figure 7. Dependence of activity with time on stream (TOS) for *n*-butane hydrogenolysis catalyzed by PtRu/γ-Al_2O_3.

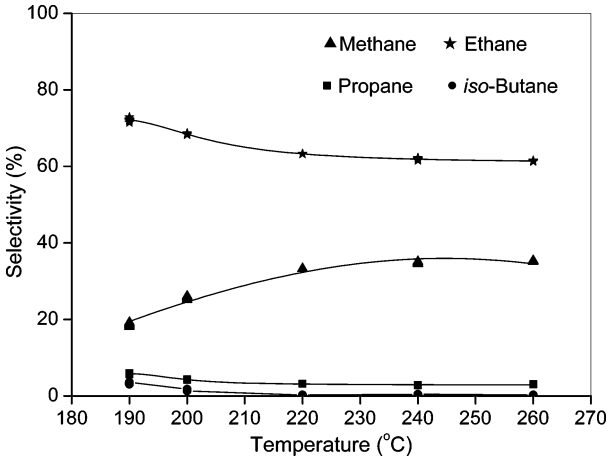

Figure 8. Dependence of selectivity on reaction temperature for *n*-butane hydrogenolysis catalyzed by PtRu/γ-Al_2O_3.

Discussion

IR Evidence of Interactions between Cluster Precursor and γ-Al_2O_3. The carbonyl bands in the IR spectra show that $Pt_3Ru_6(CO)_{21}(\mu_3\text{-H})(\mu\text{-H})_3$ was adsorbed essentially intact on γ-Al_2O_3, becoming somewhat distorted and interacting with the surface primarily via CO−ligand−OH group combinations. The changes of the support OH bands show that the adsorption involved interactions of the clusters with support OH groups, presumably by hydrogen bonding; however, the carbonyl oxygen atom was only slightly polarized, and the hydrogen bonds are inferred to have been weak. We suggest that the interaction between the metal atoms in the clusters and support oxygen atoms might have had more influence on the changes of carbonyl bands than the hydrogen bonds. When metal atoms accept electron from support oxygen atoms, they have an increased tendency to back-donate electron density to empty π^* orbitals of carbonyl carbon atoms, resulting in weakened C−O bonds and causing the shift of the ν_{CO} bands to lower frequency.

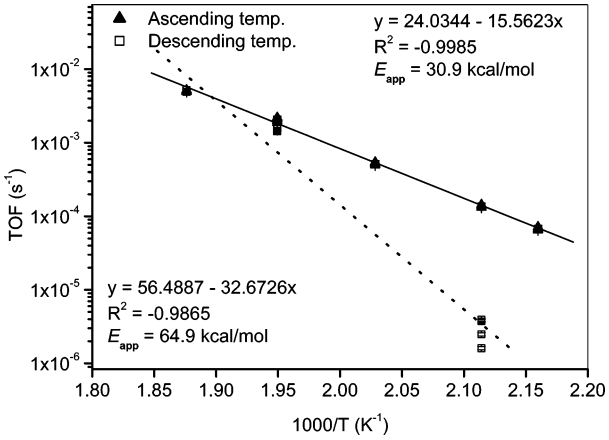

Figure 9. Arrhenius plots characterizing *n*-butane hydrogenolysis catalyzed by PtRu/γ-Al_2O_3; the TOF values represented here are approximate, because the conversions were not all differential, and the data demonstrated deactivation of the catalyst.

The IR spectrum of the dried sample after the attempted extraction with CH_2Cl_2 (Figure 1b, spectrum 2) closely resembles that of the freshly prepared sample, indicating that the adsorbed species remained stably adsorbed. The tight binding of the precursor to the support, combined with the evidence summarized above indicating retention of the cluster frame, demonstrates the preparation of strongly adsorbed clusters from which ligands might be removed without substantial breakup of the metal frame or aggregation of the metal.

EXAFS Evidence of Interactions between Cluster Precursor and γ-Al_2O_3. The EXAFS parameters indicating cluster−support interactions (Table 1) represent average $M-O_{support}$ distances and coordination numbers (where M is Pt or Ru). The interactions are characterized by both short and long metal−oxygen contributions ($M-O_s$ and $M-O_l$). We infer that the interactions between the metal and support oxygen atoms helped to maintain the cluster dispersed on the support. The average $Pt-O_s$ distance was 2.55 ± 0.01 Å with a coordination number 1.8 ± 0.1, and the average $Ru-O_s$ distance was 2.34 ± 0.01 Å with a coordination number of 1.4 ± 0.1. Both distances are longer than the 2.26 ± 0.01 and 2.13 ± 0.01 Å for $Pt-O_s$ and $Ru-O_s$ reported previously for a cluster lacking hydride ligands, $Pt_2Ru_4(CO)_{18}$, adsorbed on γ-Al_2O_3.[6] These $Ru-O_s$ distances are longer than that characterizing $Ru_3(CO)_{12}$ on γ-Al_2O_3 (2.17 Å).[32]

These observations agree with the inference based on electron counting that the metal core of the precursor with hydride ligands, $Pt_3Ru_6(CO)_{21}(\mu_3\text{-H})(\mu\text{-H})_3$, was coordinatively saturated and interacted more weakly with oxygen atoms of the γ-Al_2O_3 than the metal core of $Pt_2Ru_4(CO)_{18}$, which was not coordinatively saturated.[33] We infer that the distances between the metal atoms and the support oxygen atoms were relatively long because the metal frame was surrounded by carbonyl ligands, which prevented closer contact. Consistent with this inference, these distances became smaller when the CO ligands were removed, as discussed below.

The data also indicate changes in the average distances and coordination numbers of the M−CO bonds resulting from the

adsorption. The $M-O_{support}$ interactions between the precursor and γ-Al_2O_3 were evidently sufficient to lengthen some C−O bonds (with a corresponding observed increase of the Pt−O* distance). The data of Table 1 show that the Pt−C and Ru−C distances and coordination numbers characterizing the adsorbed species were similar to those in the crystalline precursor (bond distance 1.85 ± 0.01 and 1.88 ± 0.01 Å, respectively). The average Pt−O* distance in the adsorbed species was 3.09 ± 0.01 Å, longer than the distance in the unsupported crystalline form (2.99 Å, Table 1).[13]

In summary, the comparison indicates that the precursor adsorbed strongly on the support, and on the basis of the preceding discussion we infer two types of interactions: those between the metal and support oxygen atoms and those between carbonyl oxygen atoms and support OH groups.

In contrast to the Pt−CO contributions, the Ru−CO contributions did not change significantly as a result of adsorption. Ru−C and Ru−O* interactions were observed at distances of 1.88 ± 0.01 and 3.00 ± 0.01 Å, respectively, with coordination numbers of 3.1 ± 0.1. Interpretation of the Ru−CO contributions is inferred to be complicated by changes of the hydride ligands upon adsorption (see the next section).

Structure of the Cluster Frame after Adsorption. Table 1 shows a comparison of the bond distances and coordination numbers of $Pt_3Ru_6(CO)_{21}(\mu_3\text{-H})(\mu\text{-H})_3$ (determined crystallographically[13]) with those of the adsorbed clusters determined by EXAFS spectroscopy. The most significant result is that the metal−metal coordination numbers indicate that the metal core of the precursor was essentially intact in the adsorbed clusters. The essentially unchanged Pt−C and Ru−C coordination numbers indicate the lack of decarbonylation. The average Pt−Pt and Pt−Ru distances increased upon adsorption, from 2.64 to 2.68 Å and from 2.80 to 2.95 Å, respectively. The cluster expansion might have been caused by the interactions of Pt atoms with the support oxygen atoms. In contrast, the average Ru−Ru distance decreased from 3.04 to 2.83 Å. We suggest that the shortening of the average Ru−Ru distance was the result of loss of hydride ligands attached to a Ru_3 face and Ru−Ru edges; the new Ru−Ru distance is similar to the average Ru−Ru distance of the hydride-free Ru_3 face of $Pt_3Ru_6(CO)_{21}(\mu$-CPhCHPh)(μ-H), 2.81 Å.[13]

Removal of the hydrides would have provided empty coordination sites on Ru to allow their interaction with the support. The comparatively short Ru−O distance of 2.34 Å supports this statement. Again, we expect that the interaction was hindered by carbonyl ligands and became stronger upon decarbonylation of the clusters.

The changes in average metal−metal distances were different from those observed for the physisorption of $Pt_2Ru_4(CO)_{18}$,[6] corresponding to its lack of hydride ligands; the metal−metal distances of the adsorbed clusters nearly matched those of the precursor. The stronger precursor−support interaction could have resulted from partial decarbonylation to provide empty coordination sites on the metals.

Our results, in contrast, show that a cluster precursor that incorporates hydride ligands offers the opportunity for cluster chemisorption associated with loss of hydride ligands instead of carbonyl ligands.

Evidence that Supported Clusters were Chemisorbed. To repeat, a number of results support the inference that there were strong interactions between the precursor and support: the shifting of the carbonyl bands of the precursor to lower frequencies; the decrease in the intensity of bands representing support OH groups; the lack of significant extraction of the adsorbed precursors; and the interactions between the metals and support oxygen atoms indicated by the EXAFS data. The shift of the carbonyl bands to lower frequency indicates weakening of the C−O bonds, which could be the result of interactions between the carbonyl oxygen and support (e.g., support OH groups) and/or donation of electron density by support oxygen atoms to the metals, resulting in increased back-donation of electron density from the metal to π* orbital on carbon.

In summary, the IR and EXAFS data show that the adsorption of $Pt_3Ru_6(CO)_{21}(\mu_3\text{-H})(\mu\text{-H})_3$ on γ-Al_2O_3 gave chemisorbed species similar to the cluster precursor but with some distortions that are indicative of the adsorbate−support bonding.

Stability of the Metal Frame in Decarbonylated Clusters. A principal goal of this research was to prepare supported bimetallic clusters that were nearly uniform (with the metal frames intact) and highly dispersed on the support while no longer incorporating the original ligands. Because the metals in metal carbonyl precursors are typically present in low oxidation states, the activation to remove these ligands can often be carried out under mild conditions, with the prospect of leaving the metals in a reduced state. Supported bimetallic clusters prepared in this way offer the prospect of being highly selective catalysts, associated with their near uniformity of structure.[6−9]

Characterization of the decarbonylated clusters by EXAFS spectroscopy provides evidence of any changes in the metal frame. The data show that as a result of the decarbonylation the Pt−Pt bond distance decreased from 2.68 to 2.64 Å and the Ru−Ru distance decreased from 2.83 to 2.62 Å. The average Pt−Ru (and Ru−Pt) bond distances (i.e., those determined from the EXAFS data at the Pt (and Ru) edges, respectively) decreased, from 2.95 to 2.68 Å, but, most important for our goals, the Pt−Pt and Ru−Ru coordination numbers changed only barely (if at all, in view of the errors in the data). Specifically, the values changed from 2.2 ± 0.1 to 1.7 ± 0.2 and from 1.9 ± 0.1 to 2.1 ± 0.1, respectively. These results indicate that metal core was quite stable upon decarbonylation, with the metal frames remaining essentially intact, with no evidence of substantial aggregation of the metal on the support. This is the first example of such structurally simple and uniform bimetallic clusters with the original ligands removed.

However, we emphasize that the coordination number representing the Pt−Ru and Ru−Pt contributions decreased from 3.9 ± 0.1 to 2.2 ± 0.1 and from 2.0 ± 0.1 to 1.0 ± 0.1, respectively, indicating that metal−metal bonds were broken during the decarbonylation. The changes in the Pt−Ru and Ru−Pt coordination numbers show that the bimetallic frames were restructured as a result of the decarbonylation, presumably to accommodate increased interactions with the γ-Al_2O_3 surface.

Models of the resultant bimetallic clusters are proposed on the basis of the Pt−Pt, Pt−Ru, Ru−Ru, and Ru−Pt coordination numbers (Table 2) (recall that the errors in these values are approximately ±20%). Metal atoms were presumed to be in a reduced state after decarbonylation. Because the atomic radii of Pt and Ru are almost the same, namely, 1.38 and 1.34 Å, respectively,[35] a nearly close packing of the metal atoms in the model clusters was taken as an appropriate approximation. We caution that the data are not sufficient to determine the exact cluster structures and that the presence of mixtures cannot be excluded.

After removal of the carbonyl ligands, the metal atoms had more empty coordination sites and could form stronger bonds with the electronegative surface oxygen atoms. The average Pt−O_s distances decreased from 2.55 Å in the adsorbed metal

carbonyl species to 2.08 Å (with a coordination number of 2.2) in the decarbonylated sample. The latter distance indicates Pt−O_s bonds, which are typical of supported platinum-group metal catalysts.[32] The Pt−O_s coordination number increased somewhat, from 1.8 ± 0.1 to 2.2 ± 0.1, indicating that the triangular Pt_3 unit might have tilted to the support to increase interaction with support oxygen. The average Ru−O_s distance also decreased, from 2.34 to 2.06 Å. Furthermore, Ru−O distances longer than normal Ru−O bond distances were observed, namely, Ru−O_l at 2.89 Å and Ru−O_{l2} at 3.32 Å. The observations imply that the Ru atoms were in a more open structure than the Pt atoms, which were located between Ru atoms (Table 2). The coordination number characterizing the Ru−O_s contribution decreased only insignificantly, from 1.4 ± 0.1 to 1.2 ± 0.1. The Pt−O_s coordination number is greater than the Ru−O_s coordination number, indicating that some Ru atoms might have been positioned next to other metal atoms within the cluster. Thus, models II and IV in Table 2 are inferred to be more appropriate than models I, III, and V.

The total coordination number characterizing groups bonded to Pt was not significantly different from that of Pt atoms in the crystalline form of the precursor or from that characterizing the metal carbonyl on γ-Al_2O_3 before decarbonylation; the corresponding values for Ru are lower than those of the crystalline precursor and the adsorbed metal carbonyl. Therefore, we infer that there was no significant aggregation of metal resulting from decarbonylation in He at 300 °C; these treatment conditions were evidently not severe enough to break all of the Pt−Ru bonds.

Catalysis of Ethylene Hydrogenation. Both the catalyst synthesized from the bimetallic precursor and that prepared from the separate monometallic precursors were active for ethylene hydrogenation. The activities of two samples were not significantly different from each other (Table 3). This catalytic test reaction was chosen because it takes place at low temperatures and minimizes the likelihood of structural changes in the catalysts, but because both of the individual metals are catalytically active for this reaction,[36−40] it does not provide a strong basis for discrimination between the two classes of bimetallic catalyst. Consistent with this statement, the temperature dependence of the reaction rates (turnover frequencies) observed in our work was in the same range as had been observed for PtRu catalysts prepared from $RuPt_2(CO)_5(PPh_3)_3$ supported on a polymer,[37] a catalyst prepared from a mixture of $Pt(acac)_2$ and $Ru(acac)_3$ or $Pt(cod)Cl_2$ and $Ru(cod)Cl_2$ (cod is cyclooctadienyl) supported on γ-Al_2O_3,[36] and platinum supported on Al_2O_3.[38,39]

Catalysis of *n*-Butane Hydrogenolysis. The hydrogenolysis reaction, in contrast to the hydrogenation reaction, is structure-sensitive and expected to provide a better basis for discrimination between bimetallic catalysts with different structures. Our data show that the selectivity for formation of ethane, propane, and *iso*-butane decreased slightly with reaction temperature, whereas that for formation of methane increased slightly. These results imply an increasing tendency for sequential hydrogenolysis, converting the higher alkanes into methane, at higher temperatures.

The small amount of *iso*-butane obtained from *n*-butane hydrogenolysis catalyzed by Pt−Ru/γ-Al_2O_3 suggests that the isomerization reaction was suppressed when Pt atoms were incorporated with Ru in Pt−Ru/γ-Al_2O_3. Similar results were observed for *n*-butane hydrogenolysis catalyzed by RhPt catalysts supported on mesoporous FSM-16 and HMM-1, which gave 82% ethane selectivity at 200 °C.[41] Addition of Pt to Rh helped facilitate the central C−C bond cleavage reaction. High selectivity for ethane, suggesting that bonding of *n*-butane occurred mainly through 2,3-adsorption, was reported for RhPt/SiO_2.[42] The main *n*-butane hydrogenolysis reaction on RhPt/SiO_2 was central-bond cleavage to form ethane, with methane and propane resulting from terminal-bond cleavage or 1,2-adsorption. Thus, our data suggest that most of that *n*-butane bonded to the bimetallic catalyst as 2,3-adsorbed species giving ethane as the main product, rather than 1,2-adsorbed species. However, the data do not exclude multiple hydrogenolysis, consistent with the observed higher selectivity for methane than propane.

Conclusions

$Pt_3Ru_6(CO)_{21}(\mu_3\text{-H})(\mu\text{-H})_3$ was used as a precursor to prepare supported bimetallic clusters on γ-Al_2O_3. Chemisorption of the precursor followed by decarbonylation led to bimetallic clusters on the support with a metal frame essentially the same size as that of the precursor. The hydride ligands on the precursor are inferred to facilitate its simple chemisorption. As the CO ligands were removed from the adsorbed clusters by treatment in He at 300 °C, the metals interacted more strongly with the support, accompanied by some change in the structure of the metal frame, as characterized by EXAFS spectroscopy. Models of the supported clusters are presented in Table 2. These supported bimetallic clusters are evidently the first with metal frames matching those of a bimetallic precursor and structurally the best-defined supported bimetallic catalysts.

Acknowledgment. We thank N. E. Schore of the University of California, Davis, for access to the synthesis equipment. Financial support for S.C. was provided by the Ministry of University Affairs and Prince of Songkla University, Pattani Campus, Thailand; support was also provided by the Petroleum Research Fund, administered by the American Chemical Society, Grant 39484-AC3.

References and Notes

(1) *Catalytic Naphtha Reforming*; Antos, G. A., Aitani, A. M., Parera, J. M., Eds.; Marcel Dekker: New York, 1995.
(2) Shelef, M.; Graham, G. W. *Catal. Rev.—Sci. Eng.* **1994**, *36*, 433.
(3) *Handbook of Fuel Cells*; Vielstich, W., Lamm, A., Gasteiger, H. A., Eds. Wiley: West Sussex, 2003.
(4) Sinfelt, J. H. *Bimetallic Catalysts. Discoveries, Concepts, and Applications*; Wiley: New York, 1983.
(5) Sinfelt, J. H. *Acc. Chem. Res.* **1987**, *20*, 134.
(6) Alexeev, O.; Graham, G. W.; Shelef, M.; Adams, R. D.; Gates, B. C. *J. Phys. Chem. B* **2002**, *106*, 4697.
(7) Braunstein, P.; Rose, J. In *Catalysis by Di- and Polynuclear Metal Cluster Complexes*; Adams, R. D., Cotton, F. A., Eds.; VCH: New York, 1998; p 443.
(8) Alexeev, O.; Gates, B. C. *Ind. Eng. Chem. Res.* **2003**, *42*, 1571.
(9) Bergmeister, J. J.; Hanson, B. E. *Organometallics* **1989**, *8*, 283.
(10) Adams, R. D.; Alexander, M. S.; Arafa, I.; Wu, W. *Inorg. Chem.* **1991**, *30*, 4717.
(11) Adams, R. D.; Wu, W. *J. Cluster Sci.* **1991**, *2*, 271.
(12) Adams, R. D.; Chen, W.; Wu, W. *J. Cluster Sci.* **1993**, *4*, 119.
(13) Adams, R. D.; Barnard, T. S.; Li, Z.; Wu, W.; Yamamoto, J. *Organometallics* **1994**, *13*, 2357.
(14) Niemantsverdriet, J. W. *Spectroscopy in Catalysis*, 2nd ed.; Wiley-VCH: Weinheim, 2000.
(15) Nasher, M. S.; Frenkel, A. I.; Adler, D. L.; Shapley, J. R.; Nuzzo, R. G. *J. Am. Soc.* **1997**, *119*, 7760.
(16) Nasher, M. S.; Frenkel, A. I.; Somerville, D.; Hills, C. W.; Shapley, J. R.; Nuzzo, R. G. *J. Am. Chem. Soc.* **1998**, *120*, 8093.
(17) Hills, C. H.; Nasher, M. S.; Frenkel, A. I.; Shapley, J. R.; Nuzzo, R. G. *Langmuir* **1999**, *15*, 690.
(18) Jentoft, R. E.; Deutsch, S. E.; Gates, B. C. *Rev. Sci. Instrum.* **1996**, *67*, 2111.
(19) Alexeev, O.; Panjabi, G.; Gates, B. C. *J. Catal.* **1998**, *173*, 196.
(20) Raval, B. ATHENA: EXAFS data processing, 2003; http://feff.phys.washington.edu/~ravel/software/exafs/aboutathena.html (accessed December 1, 2003).

(21) http://www-ssrl.slac.stanford.edu/exafspak.html (accessed March 14, 2004).

(22) Rehr, J. J.; Mustre de leon, J.; Zabinsky, S. I.; Albers, R. C. *J. Am. Chem. Soc.* **1991**, *113*, 5135.

(23) Liang, A. J.; Bhirud, V. A.; Ehresmann, J. O.; Kletnieks, P. W.; Haw, J. F.; Gates, B. C. *J. Phys. Chem. B* **2005**, *109*, 24236.

(24) Argo, A. M.; Odzak, J. F.; Gates, B. C. *J. Am. Chem. Soc*. **2003**, *125*, 7107.

(25) Stern, E. A. *Phys. Rev. B* **1993**, *48*, 9825.

(26) Guzman, J.; Gates, B. C. *J. Chem. Soc., Dalton Trans.* **2003**, 3303.

(27) Hadjiivanov, K. I.; Vayssilov, G. N. *Adv. Catal.* **2002**, *47*, 451.

(28) Asakura, K.; Bando, K.-K.; Iwasawa, Y. *J. Chem. Soc., Faraday Trans.* **1990**, *86*, 2645.

(29) Brown, T. L. *J. Mol. Catal*. **1981**, *12*, 41.

(30) Knözinger, H.; Ratnasamy, P. *Catal. Rev.—Sci. Eng*. **1978**, *17*, 201.

(31) Mestl, G.; Knözinger, H. In *Handbook of Heterogeneous Catalysis*; Ertl, G., Knözinger, H., Weitkamp, J., Eds.; VCH: Weinheim, 1997; Vol. 2, pp 563−569.

(32) Koningsberger, D. C.; Gates, B. C. *Catal. Lett.* **1992**, *14*, 271.

(33) $Pt_2Ru_4(CO)_{18}$ and $Pt_3Ru_6(CO)_{21}(\mu_3\text{-H})(\mu\text{-H})_3$ differ in terms of coordinative saturation of the metal cores. That of the former has 88 valence electrons,[12] lower than the value predicted by the polyhedral skeletal electron pair theory (i.e., 90 electrons).[34] The number of electrons indicates that $Pt_2Ru_4(CO)_{18}$ is coordinatively unsaturated and can interact with electron-donor groups. The metal core of the latter cluster has 124 valence electrons, which is equal to the predicted number.[13] Thus, the metal core was coordinatively saturated and interactions with electron donor groups were expected to be weak. This expectation agrees with EXAFS data, showing that the distance between the metal core and support oxygen was shorter for $Pt_2Ru_4(CO)_{18}$ than the supported clusters formed from $Pt_3Ru_6(CO)_{21}(\mu_3\text{-H})(\mu\text{-H})_3$.

(34) Mingos, D. M.; May, A. S. In *The Chemistry of Metal Cluster Complexes*; Shriver, D. F., Kaesz, H. D., Adams, R. D., Eds; VCH Publishers: New York, 1990; p 81.

(35) Emsley, J. *The Elements*, 2nd Edition; Oxford University Press: Oxford, U.K., 1991; pp 142, 166.

(36) Chotisuwan, S.; Wittayakun, J.; Gates, B. C. *Suranaree J. Sci. Technol*. **2005**, *12*, 54.

(37) Pierantozzi, R.; McQuade, K. J.; Gates, B. C.; Wolf, M.; Knözinger, H.; Ruhmann, W. *J. Am. Chem. Soc*. **1979**, *101*, 5436.

(38) Hwang, K. S.; Yang, M.; Zhu, J.; Grunes, J.; Somorjai, G. A. *J. Mol. Catal. A: Chem.* **2003**, *204−205*, 499.

(39) Grunes, J.; Zhu, J.; Yang, M.; Somorjai, G. A. *Catal. Lett.* **2003**, *86*, 157.

(40) Jordan, D. S.; Bell, A. T. *J. Phys. Chem.* **1986**, *90*, 4797.

(41) Dhepe, P. L.; Fukuoka, A.; Ichikawa, M. *Phys. Chem. Chem. Phys.* **2003**, *5*, 5565.

(42) Wong, T. C.; Chang, L. C.; Haller, G. L.; Oliver, J. A.; Scaife, N. R.; Kemball, C. *J. Catal.* **1984**, *87*, 389−397.